Massively parallelized Boundary Element simulation of voxel-based human models exposed to MRI fields

Oriano Bottauscio (*), Mario Chiampi (^), and Luca Zilberti (*)
(*) Istituto Nazionale di Ricerca Metrologica
Strada delle Cacce 91, 10135 Torino, Italy, o.bottauscio@inrim.it, l.zilberti@inrim.it
(^) Dipartimento Energia, Politecnico di Torino
Corso Duca degli Abruzzi 24, 10124 Torino, Italy, mario.chiampi@polito.it

***Abstract*—The Boundary Element Method is applied to the computation of induced electric field and specific absorption rate (SAR) in voxel-based human models undergoing magnetic resonance imaging (MRI). Due to the very large size of the algebraic system, the procedure uses an iterative GMRES solver recalculating the element matrix at each iteration. A suitable processing of the Green integrals and a massively parallelized algorithm leads to a strong reduction of the computational time.**

***Index Terms*— Boundary element methods, Electromagnetic radiation effects, Magnetic resonance imaging, Modeling.**

I. Introduction

The knowledge of human exposure to electromagnetic fields is a fundamental requirement for the analysis and optimization of solutions aimed at increasing safety in MRI environments. In this context, attention is devoted to the evaluation of compliance with regulatory limits for patients and workers. Exposure issues in MRI environment are under specific attention by ICNIRP; even if some exposure criteria have been promulgated for MRI operations, important challenges warrant further investigations [1]. In particular, recent progress in mathematical modelling has evidenced how whole-body and local SAR limits for RF power deposition can be partially inconsistent [2]. The interest towards accurate prediction of localized power deposition is also needed for the development of emerging technologies in MRI, such as parallel transmission and ultra-high fields. Even more important is the evaluation of all possible issues related to patients' safety and the reduction of artifacts when facing the extension of MRI to patients carrying medical implants [3, 4].

Since in-vivo measurements are unfeasible, efficient and reliable mathematical models, extended towards realistic body models, are needed for estimating induced effects. Anatomically and electrically detailed human models such as the Virtual Family, the HPA NORMAN and NAOMI data sets are available to calculate RF induced electric fields in humans and the great majority of numerical dosimetry studies are nowadays performed by adopting the finite difference time-domain method (FDTD) [5] or finite integration technique (FIT) [6], also thanks to the widely diffused commercial software SEMCAD [7] and CST Microwave Studio [8]. However, the validation of the simulations is a difficult task and dosimetry modeling is still considered in the field of research, not wholly relevant with regard to standardization objectives. Thus, a variety of alternative methodologies, based on different numerical techniques, have been proposed for RF and LF electromagnetic field exposure [9-12].

This is the main scope of this work, where we propose an implementation of the Boundary Element method (BEM) for voxel-based human models, adopting a different strategy with respect to the one proposed in [12]. The Boundary Element method is well suited for handling large open boundary domains, as in the study of human exposure in MRI environment. Moreover, in virtue of the Green function, it guarantees a smooth reconstruction of the solutions so that it is adopted when high accuracy in field reconstruction is needed, as for example in MRI coil design [13]. Since this technique is usually applied for studying homogeneous or weakly non-homogeneous domains, a specific implementation is needed to account for highly heterogeneous voxel-based models.

II. BEM for Voxel-based Models

Consider a 3-D human model discretized into homogeneous cubic voxels, with electric conductivity σ, electric permittivity ε and magnetic permeability μ. In the BEM application, each voxel is identified as a homogeneous volume, whose bounding surface is oriented according to a normal unit vector **n** directed inwards. We associate uniform electric (**E**) and magnetic (**H**) field unknowns over each voxel side. For the generic *i*-th elementary surface, the Electric Field Integral Equation (EFIE) and the Magnetic Field Integral Equation (MFIE), written in the frequency domain (angular frequency ω), holds:

$$\begin{aligned}\xi\mathbf{E}_i = &\int_{\Omega_s}\left(\frac{\rho}{\varepsilon}\nabla\Psi - j\omega\mu\Psi\mathbf{J}_s\right)dv - \sum_{m=1}^{M}(\mathbf{n}\times\mathbf{E})_m \times \int_{\partial\Omega_m}\nabla\Psi_{i,m}ds \\ &- \sum_{m=1}^{M}(\mathbf{n}\cdot\mathbf{E})_m \int_{\partial\Omega_m}\nabla\Psi_{i,m}ds + j\omega\mu\sum_{m=1}^{M}(\mathbf{n}\times\mathbf{H})_m \int_{\partial\Omega_m}\Psi_{i,m}ds\end{aligned} \tag{1}$$

$$\begin{aligned}\xi\mathbf{H}_i = &\int_{\Omega_s}(\mathbf{J}_s\times\nabla\Psi)dv - \sum_{m=1}^{M}(\mathbf{n}\times\mathbf{H})_m \times \int_{\partial\Omega_m}\nabla\Psi_{i,m}ds \\ &- \sum_{m=1}^{M}(\mathbf{n}\cdot\mathbf{H})_m \int_{\partial\Omega_m}\nabla\Psi_{i,m}ds - j\omega\tilde{\varepsilon}\sum_{m=1}^{M}(\mathbf{n}\times\mathbf{E})_m \int_{\partial\Omega_m}\Psi_{i,m}ds\end{aligned} \tag{2}$$

where $\partial\Omega_m$ (m=1,..M) are the surfaces which interact with surface i and ξ is the singularity factor. In Eqn. (1) and (2) the volume integrals represent the field sources (with impressed current density $\boldsymbol{J}_s$ or volume charge density ρ) located in the external open-boundary region and interacting with the only external surfaces. The Green function is expressed as:

$$\Psi = \frac{e^{-jk|\boldsymbol{r}-\boldsymbol{r}'|}}{4\pi|\boldsymbol{r}-\boldsymbol{r}'|} \quad \text{with} \quad k = \omega\sqrt{\mu\left(\varepsilon - j\frac{\sigma}{\omega}\right)} = \omega\sqrt{\mu\tilde{\varepsilon}}$$

where $\boldsymbol{r}$ and $\boldsymbol{r}'$ are the coordinate vectors of the observation and source points. For each voxel side dividing volumes (1)

and (2), thanks to the field interface conditions, we assume as complex unknowns (phasors) the components E_n, H_{t1}, H_{t2} on side (1) and E_{t1}, E_{t2}, H_n on side (2), being $\{\mathbf{n},\mathbf{t}_1,\mathbf{t}_2\}$ the local coordinate system and $\left|\tilde{\varepsilon}^{(2)}\right| > \left|\tilde{\varepsilon}^{(1)}\right|$. Eqn. (1) and (2), projected on $\{\mathbf{n},\mathbf{t}_1,\mathbf{t}_2\}$, are written on both sides and summed two by two to obtain six scalar equations.

Due to the high number of unknowns arising from a voxel-based model, the complex algebraic system deriving from Eqn. (1) and (2) cannot be stored in memory, enforcing the use of a GMRES iterative algorithm. Since this method requires a matrix-vector product, it can be implemented by processing one matrix row at a time instead of the whole matrix. Obviously, as a drawback, the matrix elements must be recomputed at each iteration.

To speed up the matrix element recalculations, we adopt two strategies. Firstly, since the voxel are geometrically identical, the integrals of Green function associated to the interactions among internal faces reduces to a very limited set (6 terms for each material). These terms are computed once and for all and only loaded during the iterative process. On the contrary, all the external faces interact with each other, so that the integrals associated to them cannot be restricted to a limited set, but they have to be recomputed at each iteration. The computational time can be strongly reduced through massively parallelized algorithm by implementing a multiple GPU code, based on CUDA and OpenMP libraries. In the CUDA kernel each thread computes the interactions among elementary external surfaces (a) and (b). On the basis of the characteristics of the available GPU cards (NDIVIA, Tesla M2050), a grid of $\left(L \times N / T_{\max}\right)$ blocks, with $T_{\max} = 512$ threads each, is launched on each GPU card, being N the number of external faces (source points) and $L \leq N$ a set of external faces (computational points) determined on the basis of the available memory on each card (~2.8 Gbyte for M2050).

III. Exposure to RF MRI field

The model is applied to the estimation of SAR induced in the human head as a consequence of the exposure to the RF field generated by a bird-cage coil of a 1.5 T MRI scanner (working frequency of 64 MHz). The voxel model is the head of the adult male "DUKE" of the Virtual Family data set [14], with a spatial resolution of 3 mm.

Fig. 1 shows the head model and the bird-cage coil, constituted of eight conductors supplied by unitary phase-shifted currents able to generates a quite uniform rotational RF magnetic field of about 2.8 A/m in the head volume. A cross section of the head, at the forehead height, is presented in Fig. 2, which puts in evidence the non-homogeneity of the considered structure and shows the induced SAR distribution.

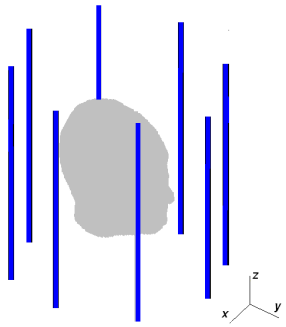

Fig. 1. "Duke" head model located within a MRI bird-cage

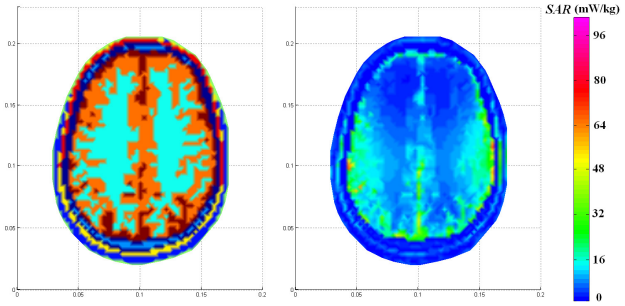

Fig. 2. Cross section at the forehead height (dimensions in meters): scheme of the materials (left); induced SAR (right).

Acknowledgment

The work was supported by EMRP grant HLT06. The EMRP is jointly funded by the EMRP participating countries within EURAMET and the European Union.

References

[1] J.C. Lin, "International Guidelines for Radio-Frequency Exposure, Especially for the Most Successful Application of Electromagnetics in Medicine: Magnetic Resonance Imaging," *IEEE Antennas and Propagation Magazine*, vol. 53, No.1, pp. 169-174, 2011.

[2] M. Zang, A. Alden, "Calculation of whole-body SAR from a 100 MHz dipole antenna," *Progress in Electromagnetics Research*, vol. 119, pp. 133-153, 2011.

[3] Y. Gao, K. Muramatsu, A. Kushibe, K. Yamazaki, A. Chiba, T. Yamamoto, "Reduction of Artifact of Metallic Implant in Magnetic Resonance Imaging by Coating of Diamagnetic Material," *IEEE Trans. on Magn.*, vol.45, no.10, pp. 4837-4840, 2009.

[4] Y. Guo, X. Jiang, "Simulations of the Stent Artifacts in Magnetic Resonance Imaging," *IEEE Trans. on Magn.*, vol. 48, no. 2, pp. 659-662, 2012.

[5] T. V. Yioultsis, et al., "A Comparative Study of the Biological Effects of Various Mobile Phone and Wireless LAN Antennas," *IEEE Trans. Magn.*, Vol. 38, No. 2, pp. 777-780, 2002.

[6] Y. Li, J. Hand et al. "Numerically-simulated induced electric field and current density within a human model located close to a z-gradient coil," *J. Magn. Reson. Imaging*, vol. 26, no.5,pp. 1286-1295, 2007.

[7] http://www.speag.com/products/semcad/overview/.

[8] CST Microwave Studio, http://www.cst.com/.

[9] H. Fahs, A. Hadjem, S. Lanteri, J. Wiart, M. Wong, "Calculation of the SAR Induced in Head Tissues Using a High-Order DGTD Method and Triangulated Geometrical Models," *IEEE Trans. on Antennas and Propagation*, vol. 59, no. 12, pp. 4669-4678, 2011.

[10] M. Lu, S. Ueno, "Dosimetry of Exposure of Patients to Pulsed Gradient Magnetic Fields in MRI," *IEEE Trans. on Magn.*, vol. 47, no. 10, pp. 3841-3844, 2011.

[11] R. Scorretti, et al., "Computation of Induced Fields Into the Human Body by Dual Finite Element Formulations," *IEEE Trans. on Magn.*, vol. 48, no. 2, pp. 783-786, 2012.

[12] S. Hamada, "GPU-accelerated indirect boundary element method for voxel model analyses with fast multipole method," *Computer Physics Communications*, vol. 182, pp. 1162-1168, 2011.

[13] G. Shou, L: Xia, F. Liu, M: Zhu, Y. Li, S. Crozier, "MRI Coil Design Using Boundary-Element Method With Regularization Technique: A Numerical Calculation Study," *IEEE Trans. on Magn.*, vol. 46, no. 4, pp. 1052-1059, 2010.

[14] Virtual family, http://www.itis.ethz.ch/news-events/news/latest-news/.